Nano Research

ISSN 1998-0124 CN 11-5974/O4
https://doi.org/10.26599/NR.2026.94908996

Review Article

High entropy nanoalloys for electrocatalytic plastic waste upcycling

Palaniappan Subramanian[1](✉), Palanisamy Kannan[2](✉), Jan Minar[1]

[1] New Technologies – Research Center, University of West Bohemia in Pilsen, 30100, Czech Republic

[2] College of Biological, Chemical Sciences and Engineering, Jiaxing University, Jiaxing 314001, China

Nano Res., **Just Accepted Manuscript** • https://doi.org/10.26599/NR.2026.94908996

https://www.sciopen.com/journal/1998-0124 on Jul. 3, 2026

Just Accepted

TABLE OF CONTENTS (TOC)

Table of Contents Artwork

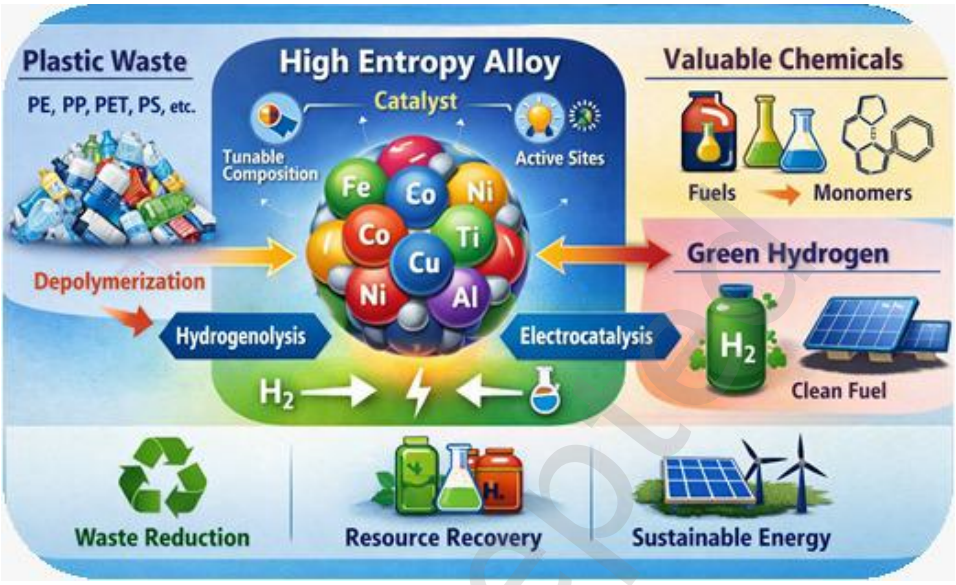

This article explores high-entropy alloy (HEA) nanostructures as electrocatalysts for converting plastic waste into valuable chemicals and fuels.

Nano Research

Open Access

Review Article

High entropy nanoalloys for electrocatalytic plastic waste upcycling

Palaniappan Subramanian[1], Palanisamy Kannan[2], and Jan Minar[1]

[1] New Technologies – Research Center, University of West Bohemia in Pilsen, 30100, Czech Republic
[2] College of Biological, Chemical Sciences and Engineering, Jiaxing University, Jiaxing 314001, China

Received: 20 April 2026; **Revised:** 12 June 2026; **Accepted:** 3 July 2026

Address correspondence to Palaniappan Subramanian, palans@ntc.zcu.cz; Palanisamy Kannan, ktpkannan@zjxu.edu.cn

Cite this article: *Nano Research*, 2026, 19, 94908996 https://doi.org/10.26599/NR.2026.94908996

ABSTRACT: Plastic pollution has become a global issue due to improper management of plastic waste, posing a significant environmental burden. Microplastic pollution is also widely recognized as a health hazard, and there is an urgent need to develop methods to upcycle plastic waste into value-added chemicals and precursors. Among upcycling approaches, electrocatalytic upcycling is gaining attention as a key technology for converting waste plastics, such as polyethylene terephthalate, polyethylene, and polystyrene, into value-added chemicals and fuels. High-entropy alloy (HEA) nanostructures are an emerging class of nanomaterials with five or more elements in near-equimolar ratios, which support catalytic oxidation of complex reactions involving plastic hydrolysate. In this review, we first focused on high-entropy alloy nanostructures that have been employed as electrocatalysts for the oxidation of plastic hydrolysate derived from various plastic wastes. We have specifically highlighted the product selectivity and conversion efficiency attained due to the availability of multi-metal HEA nanostructures. The influence of HEA dimensionality, size, and multi-site synergism on the electrocatalysis of plastic waste hydrolysates, including ethylene glycol, lactic acid, and glycolic acid, is discussed in detail. The stability aspects of HEA nanostructures, along with their performance in lab-scale test setups such as H-Cell and flow cell, are summarized. This review also outlines the challenges that need to be addressed to further develop active, stable HEAs and presents the future prospects of the electrocatalytic upcycling process for wide-scale adoption.

KEYWORDS: high-entropy alloy catalysts, multimetallic components, green hydrogen, plastic waste upcycling, value-added products, sustainability.

1. Introduction

The global issue of plastic waste has reached a critical point. over 400 million metric tons are produced annually, yet less than 10% is recycled worldwide.[1-3] Traditional mechanical recycling is limited to a few types of plastics, mainly polyethylene terephthalate (PET) and high-density polyethylene (HDPE) bottles, which together account for less than 12% of post-consumer waste. Moreover, these methods often lead to "downcycling," in which the material's quality diminishes over time, eventually necessitating disposal methods such as landfilling or incineration.[4,5] Plastic waste upcycling has emerged as a promising research field aimed at overcoming these challenges by transforming discarded materials into products with greater value or functionality.[6-8] The research values of plastic upcycling are defined by several key economic, environmental, and technological pillars.[9,10] Upcycling generates high-value products, such as impurity-free polymers, synthetic fuels, and industrial raw materials.[11] Upcycling systems using electro,[12-17] photo,[18-20] and photoelectrocatalytic[21] approaches are more favorable than incineration, with research indicating a 69-75% reduction in greenhouse gas (GHG) emissions.[21] Research efforts now focus on navigating the "chemical toolbox" to optimize structure-activity-selectivity relationships, often utilizing machine learning and process optimization to scale these solutions for industrial adoption.

HEAs represent a revolutionary shift in heterogeneous catalysis by integrating five or more metallic elements to form a "universal catalyst" framework with almost limitless design potential.[22-24] Their technological importance is anchored in the four core effects (i) high configurational entropy (ii) significant lattice distortion (iii) slow diffusion, and (iv) the synergistic "cocktail effect," which together stabilize durable single-phase solid solutions and create distinctive local electronic structures.[25-27] This complexity enables HEAs to overcome the linear scaling relationships that limit traditional catalysts by providing a varied surface landscape where different reaction intermediates can bind independently to their optimal sites.[25-27] As a result, HEAs facilitate highly efficient and selective pathways for complex multi-electron reactions such as carbon dioxide reduction (CO_2RR), nitrogen reduction (NRR), and water splitting.[28-30] Additionally, the slow diffusion effect ensures remarkable long-term durability against leaching and particle coarsening in challenging industrial settings, while their compositional adaptability allows for a significant reduction in the use of costly noble metals without compromising catalytic performance. The dimensionality of HEA nanomaterials plays a pivotal role in determining their electrocatalytic efficiency.[31-34] Transitioning from bulk materials to zero-dimensional (0D) nanoparticles, one-dimensional (1D) nanowires, or three-dimensional (3D) porous structures markedly enhances the surface-to-volume ratio and increases the density of active sites available for catalysis.[31,32] Certain morphologies, such as subnanometer nanowires or nanoporous networks, further

enhance performance by facilitating mass and charge transport and providing short diffusion pathways for reaction intermediates.[35-37] In high-entropy alloy (HEA) nanostructures, the catalytic efficiency is determined by both specific elements for reactions and common structural attributes. For ethylene glycol oxidation, platinum (Pt) and palladium (Pd) are the main active sites, while secondary elements such as iron (Fe), cobalt (Co), nickel (Ni), and manganese (Mn) require a face-centered cubic (FCC) structure and a flocculent or branched morphology.[38] In contrast, for the oxidation of lactic and glycolic acids, copper (Cu) and nickel (Ni) are the primary active sites, effectively interacting with oxygen-containing monomers. Disordered FCC/BCC phases, nanoscale morphology, and diverse local atomic environments result in unique active site distributions that transcend traditional scaling relations, thereby enabling superior multi-reaction catalysis.[38] The appropriate dimensionality is determined by the nature of the reaction: 0D or 1D configurations are ideal for EGOR and lactic acid oxidation processes, 2D configurations are best suited for oxidations sensitive to surface interactions, and three-dimensional configurations are essential for systems that produce hydrogen in tandem with multiple concurrent reactions.[39]

Electrocatalytic methods for upcycling plastic waste are favored over conventional techniques because they function under mild conditions, such as ambient temperature and pressure, and utilize eco-friendly renewable energy sources like solar and wind. This approach also boasts significantly higher energy efficiency by employing coupled anodic-cathodic reactions that generate valuable chemicals at both electrodes.[40] Electrocatalysis achieves high transformation efficiency and selective product formation by allowing precise control over chemical reactions through potential, current density, and catalyst design. This process converts plastic waste into high-value-added chemicals, such as acetic acid and terephthalic acid, instead of low-value fuels or uncontrolled degradation products.[41-43] Furthermore, unlike mechanical recycling, which requires high purity and complex pre/post-treatments, electrocatalytic upcycling can handle less purified feedstocks when combined with chemical depolymerization. This makes it a sustainable and promising method for directly converting waste plastics into valuable chemicals with low energy consumption. Electrocatalysis for plastic waste upcycling utilizes electrical energy to break down polymer chains into valuable chemicals and fuels, such as hydrogen (H_2), formate, glycolic acid (GA), and acetate (Fig. 1). HEAs and their derivatives play a crucial role in this area by providing efficient, stable, and cost-effective electrode materials that can manage the complex, multi-step reactions involved in polymer degradation.[44-46] The effectiveness of HEAs in electrocatalytic upcycling is attributed to their high configurational entropy and significant lattice distortion, which result in a heterogeneous surface with a nearly continuous range of adsorption energies.[47,48] In multi-electron processes such as plastic oxidation, HEAs can separate reaction intermediates (e.g., *CO, *CHO) that are usually bound on pure metal surfaces, enabling the reaction to approach its theoretical maximum activity.[49,50] The "cocktail effect" allows different elements within the HEA to perform specific roles simultaneously - one element may aid in water dissociation while adjacent sites stabilize intermediates derived from plastics.[51,52] Research using the high entropy oxide TiZrHfTaNbO has shown superior activity compared to benchmark TiO_2 for converting PET bottles and microplastics into H_2, terephthalate, ethylene glycol (EG), and formic acid (FA).[53] High-entropy metal tungstates (e.g., $FeCoNiCuZnWO_4$) have been demonstrated to significantly improve the selectivity and production rate of acetic acid from plastic waste by adjusting the energy band structure and *d*-band center.[54] HEAs offer a robust, corrosion-resistant platform that withstands the harsh electrolytes used in electrochemical recycling. They represent a shift from trial-and-error alloying to data-guided catalyst discovery, providing a scalable path toward a circular economy where plastic waste serves as a feedstock for green H_2 and premium industrial chemicals.

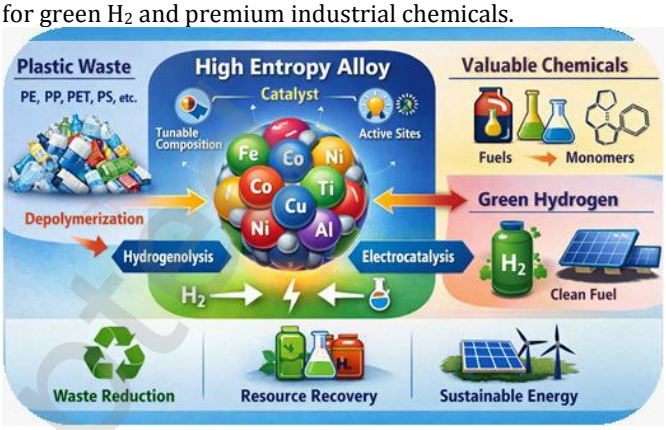

Fig. 1 High entropy nanoalloy catalysts used in the context of the electrocatalytic plastic waste upcycling process.

Plastics suitable for hydrolysis are exclusively polyesters containing hydrolyzable ester bonds (-COO-), such as PET, which depolymerizes into terephthalic acid and ethylene glycol; PLA, which converts into acetic acid; PBS, which yields succinic acid and 1,4-butanediol; and PGA, which hydrolyzes into glycolic acid. In contrast, polymers such as PE, PP, and PS are inherently difficult to depolymerize due to their inert C–C backbones, which resist both hydrolysis and electrochemical activation. It is crucial to include both categories of high-entropy alloys viz., noble-metal HEAs (based on Au, Pt, Ni) exhibit superior activity and selectivity for complex transformations, whereas noble-metal-free HEAs (based on Cu, Fe, Co, Ni, Zn) offer scalability and cost-effectiveness. Only water-soluble monomer fragments have been demonstrated for electrocatalytic transformation using HEA nanomaterials. Therefore, this review only focuses on plastic waste amenable to pre-hydrolysis or depolymerization to form water-soluble monomers. The following section presents a condensed review of dimensionally varied HEA nanomaterials developed for upcycling of hydrolysable plastic waste via an electrocatalytic approach.

2. 0D High entropy alloy nanomaterials

0D HEA materials are composed of several (normally five or more) main elements mixed in almost equal atomic proportions. At the atomic level, they form distinctive structures and their 0D nature refers to forms like nanoparticles or quantum dots. Their high entropy and atomic complexity work together to give them excellent properties, such as great strength, stability, and the capability to perform better in a wide range of applications.[55,56] For instance, Chen et al.

designed a highly dispersed PtBiCoAgSn electrocatalyst to effectively convert waste plastic-derived EG into valuable chemicals, such as GA.[57] Conventional Pt catalysts are often limited by their high cost and rapid deactivation. In contrast, this innovative multi-component alloy (MCA) design capitalizes on the synergistic interactions among five elements (Pt, Bi, Co, Ag, and Sn) with diverse atomic sizes and electronegativities.[57] The material is distinguished by a heterogeneous structure, where a Pt-based MCA phase coexists with AgSn alloy and Bi_2O_3 phases, resulting in lattice mismatches that are pivotal to its superior catalytic performance. The MCA-PtBiCoAgSn catalyst is characterized by its highly dispersed 0D spherical nanoparticles, averaging 5.72±2.93 nm in size, and following an approximately Gaussian distribution. This small particle size and extensive dispersion on the carbon support are pivotal in disrupting contiguous Pt-Pt bonds, thereby promoting the selective oxidation of EG through the C2 pathway.[57] Moreover, the catalyst exhibits notable lattice mismatches, with spacings between 0.233 and 0.279 nm, and significant lattice distortion due to the varied atomic sizes of its five constituent elements: Pt, Bi, Co, Ag, and Sn (Fig. 2A). These structural and dimensional characteristics induce electronic modulation that alters the *d*-band center of Pt, increases the exposure of active sites, and fosters a synergistic interaction that significantly enhances mass activity and tolerance to CO poisoning.

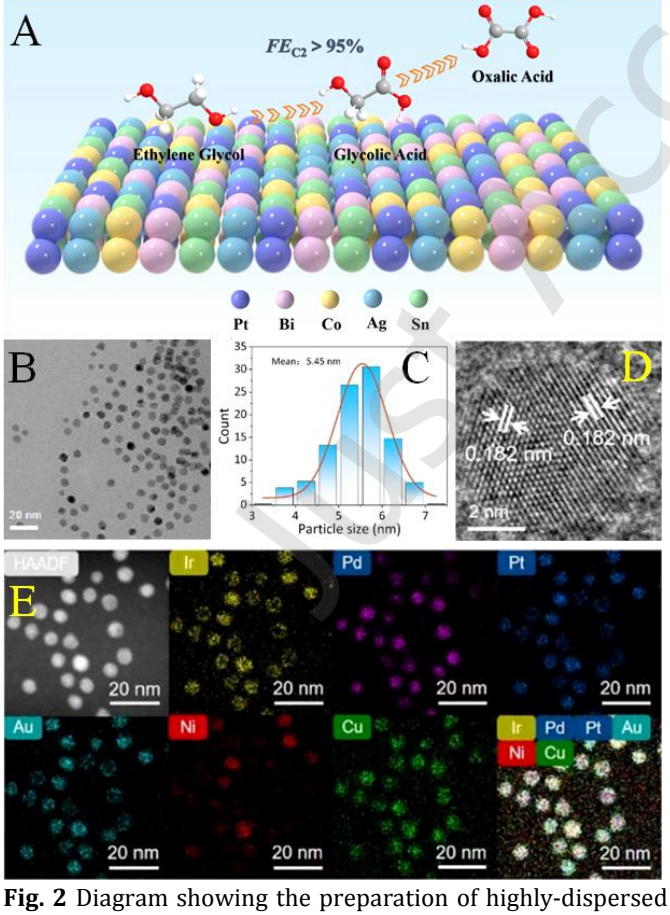

Fig. 2 Diagram showing the preparation of highly-dispersed (A) carbon-supported PtBiCoAgSn MCA catalyst for EGOR reaction. (B-E) TEM image, the size distribution, HR-TEM image, and elemental mapping of Ir-PdPtAuNiCu HEANs for EGOR reaction. Reproduced with permission from ref.[57,58] Copyright 2025 MDPI and 2025 RSC.

The MCA-PtBiCoAgSn catalyst displays exceptional electrochemical activity, achieving a mass activity for the EGOR of 16.65 A mg_{Pt}^{-1}, which is eightfold greater than that of commercial Pt/C.[57] This enhanced performance is due to electronic modulation at the atomic interfaces, which shifts the *d*-band center of Pt and lowers the activation potential by 110 mV compared to standard catalysts. Moreover, the catalyst shows improved resistance to poisoning, as the Bi_2O_3 phase produces surface hydroxyl (-OH) species that efficiently oxidize and eliminate CO-like intermediates from active Pt sites. Despite surface reconstruction and elemental leaching during extended operation, the material retains excellent stability and regenerative capability over 19 hours of cumulative testing. A key finding of the study is the catalyst's capacity to guide the reaction pathway toward high-value C2 products rather than undesirable C1 byproducts such as FA. The multi-component alloying effectively disrupts contiguous Pt-Pt bonds, promoting a preferential C2 pathway, as confirmed through in-situ electrochemical infrared spectroscopy. This structural modulation results in a Faradaic efficiency (FE) for GA of up to 91% at a low potential of 0.5 V vs. RHE.[57] Ultimately, the study concludes that precise modulation of the electronic and physical structure of MCAs offers a robust and selective strategy for the economical upcycling of organic small molecules.

Afterward, Zheng et al. synthesized small, highly dispersed PdPtAuNiCu and Ir-doped PdPtAuNiCu high-entropy alloy nanoparticles (HEANs) via a wet-chemical method to enhance the efficiency of EGOR.[58] This advancement addresses the demand for sustainable strategies to upcycle polyethylene terephthalate (PET) plastic waste into commodity chemicals such as glycolate (GA) and H_2. Unlike conventional platinum or palladium catalysts, which are prone to rapid deactivation by carbonyl intermediates, these HEANs employ multisite synergy, with the content of each element precisely balanced to optimize the electronic structure and improve stability. The catalysts are characterized by a 0D spherical nanoparticle shape with a highly uniform and small-sized distribution of 5.45 nm for the Ir-doped version and 5.50 nm for the undoped version Fig. 2B-E.[58] This ultrasmall size and high dispersion are critical to the catalyst's performance as they provide a large electrochemical surface area, maximizing the exposure of active sites and achieving a high level of atomic economy. Additionally, the well-defined spherical morphology and uniform size contribute to the catalyst's structural stability, preventing significant agglomeration even after 1200 hours of continuous high-current electrolysis.[58] This Ir-doped PdPtAuNiCu HEANs exhibit remarkable catalytic performance, achieving a mass activity of 2.41 A mg^{-1} at 0.724 V (vs. RHE) and a glycolate FE of 88.8%. In practical applications, a membrane-free flow electrolyzer utilizing this bifunctional catalyst attained an industrial-level current density exceeding 300 mA cm^{-2} and maintained ultra-stable operation for over 1200 hours without any current decline. This level of durability significantly surpasses commercial Pt/C and Pd/C benchmarks, which often deactivate within an

hour due to the accumulation of toxic intermediates on their active sites. The superior performance is attributed to the intricate interaction among the various metallic components and the specific role of the Ir dopant. The oxophilic elements, such as Ni and Au, along with oxidized metal sites, facilitate the activation of water to generate hydroxyl species (OH_{ad}), which effectively remove poisoning CO intermediates from the catalyst surface.[58] Furthermore, the incorporation of iridium induces tensile strain and electronic perturbations that shift the *d*-band center of the active sites, thereby enhancing reaction kinetics and CO-stripping capacity. The solar-driven EGOR represents a sustainable approach for converting PET plastic waste into commodity chemicals and green H_2. This process utilizes a custom-designed, membrane-free flow electrolyzer powered by an approximately 2.0 V solar panel.[58] Zheng et al., have reported the application of bifunctional Ir-doped and undoped PdPtAuNiCu HEANs as the anode and cathode, respectively, and is supplied with crude EG obtained from the alkaline hydrolysis of end-of-life PET. During a three-day outdoor trial, the setup demonstrated effective operation across varying light intensities, achieving peak productivity of 0.146 mmol h^{-1} for glycolate and 0.109 mmol h^{-1} for H_2 at a solar irradiance of 1078.1 W m^{-2}. This methodology offers a viable paradigm for storing intermittent renewable energy in value-added chemicals while concurrently addressing the environmental challenge of plastic waste management.[58]

3. 1D High entropy alloy nanomaterials

1D HEA nanomaterials are nanostructures where the components of high entropy alloys are arranged in a 1D manner for example nanowires, nanotubes, or nanorods. These materials, composed of multiple elements in almost equal proportions, show unique mechanical, electrical, and thermal properties because of their complex atomic structure and high surface area. Such materials are very promising for energy, environment, healthcare, and industry allowing new technologies and solving problems in a variety of fields including catalysis, energy, optoelectronics, sensors, etc.[59-61] For example, $L1_0$ -PtIrFeMoBi HEA intermetallic catalyst comprises nanoparticles with an average diameter of approximately 3.95 ± 1.38 nm were reported by Hao et al.[62] These nanoparticles are synthesized in-situ and anchored within 1D electrospun carbon nanofibers (CNFs), which provide a porous confined space that prevents nanoparticle aggregation and corrosion. 3D tomography reconstruction confirms that the $L1_0$ -(PtIr)(FeMoBi) nanoparticles are uniformly and densely dispersed throughout the interior and on the surface of these nanofibers. The CNF substrate itself exhibits a highly porous structure (with a measured porosity of 0.212), facilitating efficient ion-electron transport channels and expanding the active interface for catalytic reactions. The catalytic mechanism for upgrading waste plastics is centered on a multi-site synergistic effect enabled by the long-range ordered $L1_0$ structure (Fig. 3A-C).[62] In this configuration, carbonophilic Pt/Ir atomic columns serve as the primary binding sites for EG adsorption, while the oxophilic Fe/Mo/Bi columns facilitate the adsorption of hydroxyl (*OH) species. This alternating atomic configuration suppresses the competitive adsorption typically observed in conventional alloys, enabling balanced co-adsorption of EG and OH. Besides, the diluted Pt sites within the $L1_0$ -PtIrFeMoBi lattice effectively inhibit C-C bond cleavage, ensuring that the reaction primarily follows a C2 pathway to produce GA rather than C1 byproducts.[62] Density Functional Theory (DFT) studies reported in [62] indicate that this synergy significantly reduces the energy barrier to the rate-determining step, the conversion of CH_2 OH-CO intermediates into GA. In terms of performance, the PtIrFeMoBi catalyst exhibits a remarkable mass activity of 5.20 A , which is considerably higher than that of commercial Pt/C (1.4 A mg_{Pt}^{-1},) and traditional HEA solid solutions.[62] It achieves an exceptional FE of 95% for GA production, representing the most active electrocatalyst reported for selective GA synthesis. The catalyst exhibits superior stability, maintaining current density, morphology, and high FE for at least 30 hours, while commercial Pt/C rapidly declines due to intermediate poisoning. When integrated into a full electrochemical cell for EGOR-assisted H_2 production, the system requires only 0.48 V to reach 10 mA cm^{-2}, underscoring its potential for energy-efficient plastic upcycling.[62]

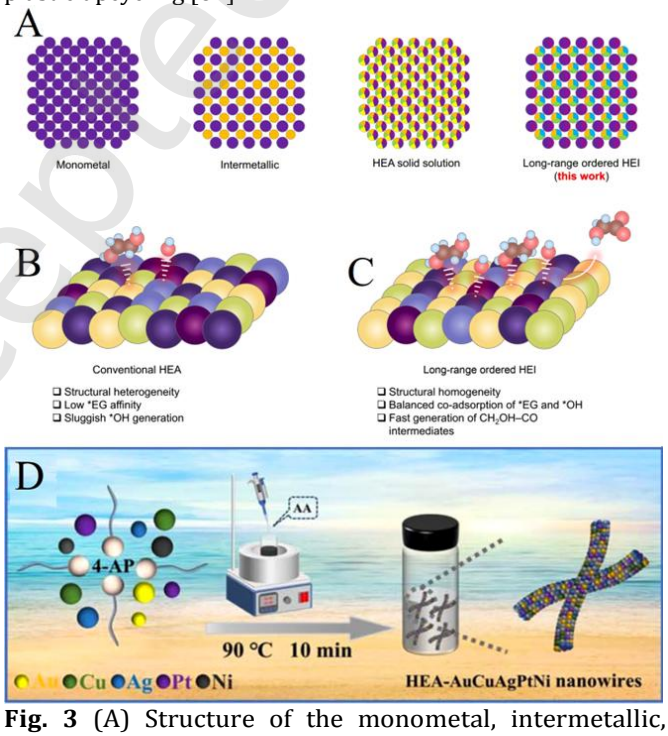

Fig. 3 (A) Structure of the monometal, intermetallic, conventional HEA, and the long-range ordered HEI. Proposed EGOR mechanism for (B) conventional HEA and (C) long-range ordered HEI. (D) Display for the synthesis of HEA-AuCuAgPtNi nanowires for LAOR process. Reproduced with permission from ref.[62,63] Copyright 2024 Wiley and 2026 RSC.

Geng et al., synthesized HEA-AuCuAgPtNi nanowires through a straightforward, one-step wet chemical process. These catalysts exhibit a distinctive morphology characterized by interconnected nanowires with an average diameter of approximately 2.1 nm and extended lengths exceeding 1.0 mm (Fig. 3D).[63] A critical attribute of these high-entropy alloy nanowires is their defect-enriched structure, which includes grain boundaries, twin boundaries, vacancy defects, and atomic steps. These structural defects, coupled with the multisite synergism inherent in the five-element system (Au, Cu, Ag, Pt, and Ni), induce lattice strain and modulate the electronic configuration. This modulation enhances charge-transfer dynamics and improves mass-

transfer efficiency by providing a high density of accessible, catalytically active sites. In performance testing within a three-electrode electrochemical system, the HEA-AuCuAgPtNi nanowires demonstrated exceptional electrocatalytic activity for the lactic acid (LA) oxidation reaction (LAOR).[63] The catalyst achieved a remarkable acetic acid yield of 115 mmol h^{-1} mg^{-1}, with 96.41% selectivity and 90.72% FE at 1.50 V vs. RHE. Compared to quaternary (AuCuAgNi, AuCuAgPt) and bimetallic (PtNi, AuPt) systems, the HEA nanowires exhibited significantly superior kinetics, as evidenced by a lower Tafel slope of 59.78 mV dec^{-1} and a larger electrochemical active surface area (ECSA) of 2.4 mF cm^{-2}.[63] Furthermore, the catalyst demonstrated high stability, maintaining its morphology and performance over 2,000 cycles and 10 hours of continuous operation, effectively converting polylactic acid plastic hydrolysate into high-value acetic acid. The proposed mechanistic pathway for converting LA to acetic acid involves a two-step process: initially, LA undergoes dehydrogenation on the catalyst surface to form pyruvic acid; subsequently, pyruvic acid is selectively oxidized, retaining its C-C bond while the carbonyl group is converted to a carboxyl group to yield acetic acid and CO_2.[63] DFT calculations reported in the above work reveal that this efficiency is driven by multisite synergism, where orbital overlaps between the five metals create multiple active sites and optimize the *d*-band electronic configuration for intermediate adsorption. To enhance economic viability, the study integrated the catalyst into a dual-function flow electrolyzer coupling anodic LAOR with the cathodic H_2 evolution reaction (HER). This integrated system operated at a significantly lower voltage than conventional water splitting, resulting in an 11.2% gain in energy efficiency while simultaneously producing high-purity H_2 with nearly 100% FE.[63]

A phosphorus-doped high-entropy carbide (P-HEC) catalyst, which is supported on electrospun carbon nanofibers (CNFs), by employing a combined electrospinning and graphitization technique at a temperature of 1000°C was prepared by Xiang and coworkers.[64] The resulting structure features randomly arranged nanofibers, each with a diameter ranging from 100 to 300 nm, which are embedded with densely and uniformly distributed P-HEC nanoparticles averaging 3.51 nm in size. The introduction of phosphorus is crucial in enhancing the catalyst's properties by generating localized electronic states that reinforce the interaction between the nanoparticles and the CNF substrate, thereby mitigating particle aggregation. Additionally, the inclusion of elements such as Fe, Co, Mn, Mo, Ni, and P alters the local electron distribution, creating an electron-deficient environment that improves EG adsorption and optimizes the electronic structure for better selectivity.[64] The mechanistic pathways of the EGOR on P-HEC/CNFs were elucidated using in-situ Raman spectroscopy and controlled electrochemical experiments, which identified nickel (Ni) as the primary active site. The reaction commences with the formation of high-valent Ni^{3+} species on the catalyst surface, which act as the main active sites. These sites promote the spontaneous dehydrogenation of EG, leading to the formation of an alkoxy intermediate, which is then oxidized into a glyoxal-like compound. The final step involves cleaving the C=C bond in this intermediate to produce FA. Concurrently, GA is generated via a Cannizzaro reaction using desorbed glyoxal. Performance evaluation in a three-electrode electrochemical cell revealed that the P-HEC/CNFs exhibit high efficiency in reforming PET-derived EG. The catalyst achieved a current density of 50 mA cm^{-2} at a low overpotential of 179 mV (relative to the oxygen evolution reaction), demonstrating an excellent current response for EGOR. It reached a peak FE of 89.25% for FA and a high yield rate of 136.46 mmol h^{-1} mg^{-1}.[64] Furthermore, the catalyst demonstrated exceptional electrochemical stability, maintaining its initial morphology and nanofiber network structure for 40 hours of continuous operation, with only minor fluctuations in current density.

4. 2D High entropy alloy nanomaterials

2D HEA nanomaterials refer to multi-element nanoscale materials in which the concentration of the constituent elements is almost equal. These are typically fabricated as thin films, nanosheets, or graphene-like layers. Due to their atomic-level complexity and large surface area, they exhibit unique properties that can significantly enhance performance in key applications such as catalysis, energy storage, and sensing.[65-68] Recently, Wang and coworkers developed turing HEA PdPtCuNiAg MARs, which are 2D, ultrathin metallene arrays featuring a periodic turing structure, synthesized in-situ on nickel foam. This self-assembled high-entropy alloy nanocrystals exhibited an average diameter of 2.0 nm, forming an ordered configuration that offers a high density of exposed active sites and a significant specific surface area (Fig. 4A).[69] The catalyst's properties are defined by the high-entropy configuration of five elements (Pd, Pt, Cu, Ni, Ag), which induces microstrain due to atomic-size discrepancies. This effect, along with electronic interactions among the metals, shifts the surface d-band centre, allowing precise tuning of intermediate adsorption strengths to prevent surface poisoning and lowering the energy barrier for the rate-determining step.

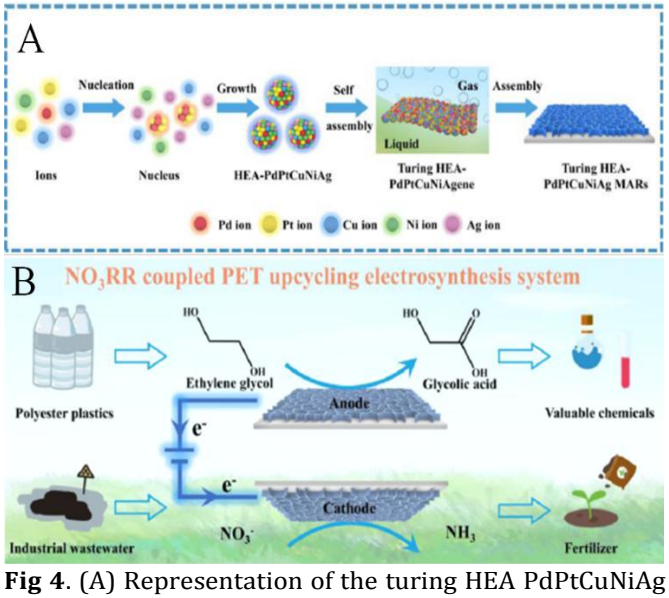

Fig 4. (A) Representation of the turing HEA PdPtCuNiAg MARs fabrication process. (B) Projected electrocatalytic combined system (NO_3RR (−) || (+) PET hydrolysate aqueous solution oxidation) for the electrocatalytic

upgrading way of PET wastes and industrial wastewater to GA and NH_3. Reproduced with permission from ref.[69] Copyright 2025 ACS.

The mechanistic pathways for dual-waste upcycling were elucidated using in-situ FTIR and DFT calculations presented in this study, demonstrating that the catalyst follows a C2 pathway for the EGOR.[69] Unlike many catalysts that cleave C-C bonds to produce CO_2, this HEA catalyst selectively oxidizes the hydroxyl group to form GA through a crucial *OC–CH_2OH intermediate, thereby avoiding over-oxidation. In the nitrate reduction reaction (NO_3RR), the catalyst operates via an NHO pathway, in which NO_3^- undergoes stepwise deoxygenation and protonation to yield ammonia (NH_3). This process is enhanced by the synergistic role of multimetallic sites: Platinum (Pt) serves as the primary active site for EGOR, Palladium (Pd) for NO_3RR, and Nickel (Ni) aids in H_2O dissociation to supply necessary *H radicals.[69] In a standard three-electrode electrochemical cell, the catalyst exhibited superior kinetics, achieving a current density of 100 mA cm^{-2} for EGOR at merely 0.67 V, which is 1.1 V lower than the oxygen evolution reaction potential. Performance analysis of a customized two-electrode membrane-electrode assembly (MEA) flow electrolyzer revealed that the coupled system (anodic PET hydrolysate oxidation and cathodic NO_3RR) achieved a high current density of 400 mA cm^{-2} at a low voltage of 1.18 V. The system demonstrated remarkable FEs for both products (FE-GA > 95.8% and FE-NH_3 > 93.4%) and maintained exceptional stability over 120 hours of continuous operation (Fig. 4B).[69] This efficiency enables the simultaneous upcycling of PET plastic and nitrate wastewater into high-purity value-added chemicals, including GA and NH_4Cl.

The PdPtRhFeCuMo high-entropy multimetallic ribbons (HMRs) are synthesized using a one-step solvothermal approach, resulting in an atomically thin, 2D nanoribbon structure with a thickness of approximately 0.7 nm. This unique morphology offers a high surface-area-to-volume ratio and extensive exposure of active sites, which are crucial for enhancing electrocatalytic efficiency.[70] As a high-entropy alloy, the catalyst benefits from a multimetallic synergistic effect and the "cocktail effect," which improve its electronic conductivity and stability. Remarkably, the PdPtRhFeCuMo HMRs display a larger electrochemical active surface area (43.7 mF cm^{-2}) compared to bimetallic alternatives and exhibit excellent resistance to CO poisoning, a common issue that typically degrades noble-metal catalysts during alcohol oxidation.[70] Mechanistically, the multimetallic synergy of the PdPtRhFeCuMo HMRs modulates the electronic structure by causing an upshift of the Pd *d*-band centers toward the Fermi level. This shift enhances the adsorption of EG and key reaction intermediates, such as 2-hydroxyacetyl (*OC-CH_2OH), which is identified as the essential precursor for converting EG to GA. DFT calculations provided in literature [70] reveal that the rate-determining step is the final deprotonation process (*OCH-CH2OH → *OC-CH_2OH).[70] The high-entropy structure effectively reduces the reaction energy barrier for this step to 1.11 eV, significantly improving the selective conversion of EG into GA while suppressing C-C bond cleavage that would otherwise lead to low-value C1 by-products. In performance analysis, the PdPtRhFeCuMo HMRs achieve a high current density of 180 mA cm^{-2} at a low potential of 0.9 V in a three-electrode system, with a peak FE of 96.81% for GA production (Fig. 5A).[70] When integrated into a two-electrode H-type electrolytic cell for PET electro-reforming, the catalyst functions as a bifunctional electrode for the co-production of GA and green H_2. At an operating voltage of 1.5 V, the system maintains high FEs of 94.97% for GA and 98.83% for H_2, demonstrating superior activity compared to conventional OER systems. Furthermore, techno-economic analysis indicates that this process is industrially viable, offering a gross profit margin of 20.6% for the upcycling of waste PET plastic into high-value chemicals.[70]

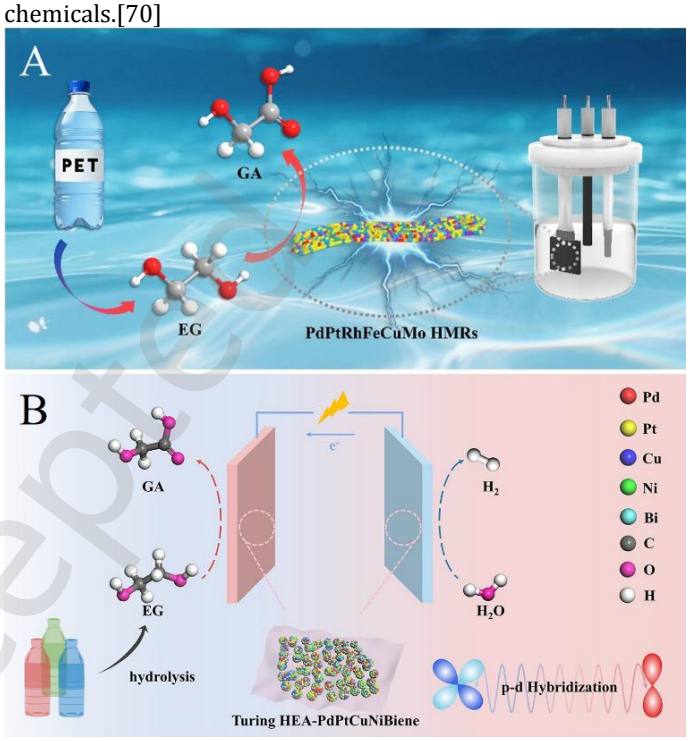

Fig 5. (A) Illustration of PdPtRhFeCuMo HMRs-based EGOR process and (B) turing HEA-PdPtCuNiBiene-based GAOR process. Reproduced with permission from ref.[70,71] Copyright 2025 and 2026, Elsevier.

An ultrathin, turing-structured PdPtCuNiBi HEA metallene (turing HEA-PdPtCuNiBiene) has been reported by Xiao et al. via a CO-induced self-assembly process at gas-liquid interfaces.[71] This 2D catalyst, measuring approximately 1.7 nm in thickness, is characterized by its intricate morphology, comprising spatially organized nanocrystals and channel-like patterns that result in a high density of electrochemically accessible active sites. The unique properties of this material stem from its high-entropy composition, which includes significant lattice strain with alternating compressive and tensile regions, as well as notable p-d orbital hybridization. This electronic configuration leads to a downward shift in the Pd *d*-band center, optimizing the adsorption strength of oxygenated intermediates and enhancing catalytic activity.[71] The catalyst's mechanistic pathways facilitate both the EGOR and HER. In the EGOR, the presence of Bi is pivotal for stabilizing key intermediates and directing the reaction towards GA production. This stabilization, coupled with a reinforced C-C bond, effectively suppresses undesirable C-C cleavage pathways that yield low-value C1 byproducts such as FA.[71] For the HER, the synergy of multiple elements and lattice distortions reduces the energy barrier to water dissociation and optimizes the free energy of H_2 adsorption, thereby accelerating reaction kinetics via the Volmer-Heyrovsky

mechanism. Performance analysis in an electrochemical cell revealed that the catalyst achieves an impressive FE of 96% for GA production at 0.9 V vs. RHE and a low HER overpotential of only 39 mV at 10 mA cm^{-2} (Fig. 5B).[71] When scaled to a two-electrode MEA flow electrolyzer, the system combined PET hydrolysate oxidation with H_2 evolution, achieving a current density of 120 mA cm^{-2} at a cell voltage of just 0.82 V. This integrated approach reduced energy consumption by 67% compared to conventional water electrolysis. The reactor demonstrated remarkable durability, maintaining structural integrity and high efficiency for over 80 hours of continuous operation, underscoring its potential for sustainable upcycling of plastic waste and cost-effective H_2 production.[71]

The study by Wang and coauthors reported HEA-PdPtSnBiAgene, a high-entropy alloy catalyst synthesized via solvothermal synthesis. This catalyst exhibits a distinctive 2D ultrathin nanosheet morphology, also referred to as "metallene," induced by in-situ-generated CO during synthesis, thereby inhibiting growth along the (111) direction. This structural configuration offers a substantial surface area with numerous uncoordinated metal sites and enhanced conductivity.[72] The catalyst exhibited a single-phase solid-solution structure, marked by significant lattice distortion and robust p-d orbital hybridization. These attributes result in a synergistic electronic effect that is crucial for optimizing the adsorption behavior of reaction intermediates.[72] Performance evaluation in an electrochemical cell reveals that HEA-PdPtSnBiAgene is highly efficient for the selective reforming of PET-derived EG into GA, achieving a peak FE of 91.8% for GA at 0.91 V, significantly surpassing pure Pd metallene in both current density and selectivity. In a two-electrode reactor designed for the co-production of GA and H_2, the system operates at a remarkably low potential of 1.11 V, which is 1.74 V lower than conventional water splitting (Fig. 6A).[72] Moreover, the catalyst demonstrates excellent cycle stability with negligible degradation over multiple operations, and techno-economic analysis indicates a high economic profit margin, highlighting its potential for industrial-scale plastic upcycling. The mechanistic pathway for the EG-to-GA conversion involves a sequential oxidation process, as confirmed by in-situ electrochemical FTIR, where *adsorbed EG is deprotonated to form a 2-hydroxyacetyl before coupling with a hydroxyl group. Theoretical analyses indicate that the downward shift of the Pd *d*-band center in the high-entropy structure facilitates the easy desorption of GA, preventing over-oxidation.[72] Additionally, the synergistic electronic effect strengthens the C-C and O-H bonds of the EG molecules, thereby suppressing C-C bond cleavage and the subsequent formation of low-value C_1 by-products. The potential-determining step is identified as the initial dehydrogenation of EG, which possesses a reduced energy barrier of 0.62 eV on the HEA surface, thereby enhancing the overall reaction kinetics.[72] The m-HEA/NF catalyst is a high-entropy mesoporous film comprising Pd, Pt, Au, Ag, and Cu, synthesized on Ni foam via a soft-template-assisted approach. Structural analysis reveals a consistent 3D interconnected mesoporous architecture with a significant BET surface area of 72.08 m^2 g^{-1} and a primary pore diameter of 48 nm. The catalyst exhibits a single-phase face-centered cubic (fcc) structure, characterized by atomic-level strain and lattice expansion resulting from the integration of multiple metal species (Fig. 6B).[73] These distinctive catalyst properties, including robust electronic hybridization and charge redistribution, where Pd, Cu, and Ag serve as electron donors to Au and Pt, shift the *d*-band centers nearer to the Fermi level, thereby optimizing the adsorption energies of intermediates for both the EGOR and HER.

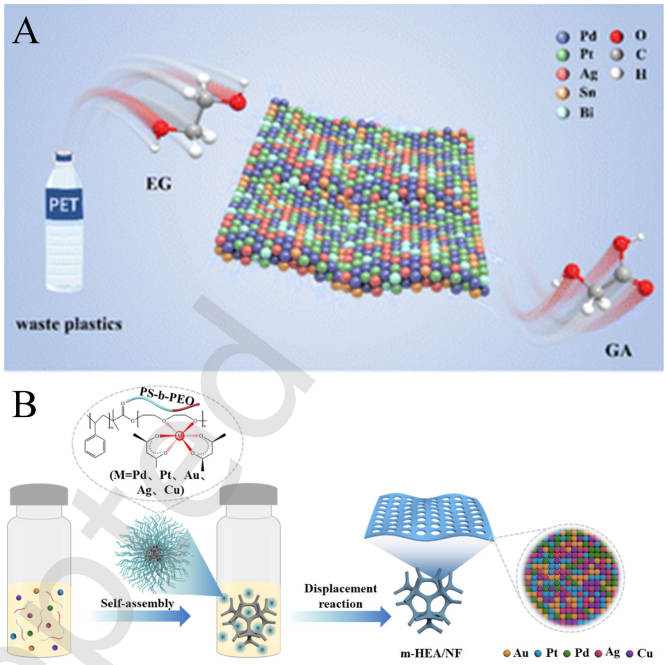

Fig. 6 (A) HEA-PdPtSnBiAgene-based EGOR process for plastic upcycling. (B) Preparation of m-HEA/NF catalyst for GAOR process. Reproduced with permission from ref.[72,73] Copyright 2025, RSC and Wiley.

The study introduces an alternating (ALT) pulse strategy to address the rapid deactivation commonly observed in noble-metal catalysts, caused by surface oxidation and intermediate poisoning.[73] Mechanistically, the ALT pulse functions through a periodic redox-regulated cycle: during anodic pulses, EG is oxidized to GA, while cathodic pulses periodically restore the active metallic sites by reducing surface metal oxides ($MO_x \rightarrow M$) and facilitating HER. In-situ Raman and FTIR spectroscopy confirm that this switching mechanism effectively prevents the accumulation of toxic carbonaceous intermediates and regenerates sites for EG re-adsorption. Theoretical calculations indicate that the multi-element synergy within the alloy reduces the energy barrier for the rate-determining step (RDS)-the dehydrogenation of *OC-CH_2OH to *GA to merely 0.487 eV, compared to 0.686 eV for pure Pd.[73] Performance evaluation in a two-electrode H-cell demonstrates that the ALT pulse system achieves a 97% FE for GA and nearly 100% for H_2 at a high current density of 250 mA cm^{-2}. The system exhibited remarkable durability, maintaining stable catalytic activity and its interconnected porous structure for 120 hours. For industrial-scale applications, a membrane-free flow electrolyzer was developed, delivering a total current of 2 A and a GA production rate of 15.114 mmol cm^{-2} h^{-1}, without cross-reactions between the anodic and cathodic products. A comprehensive techno-economic analysis highlights the commercial viability of this approach, projecting a net revenue of USD 1272.85 per metric ton of processed PET waste, effectively integrating plastic valorization with energy-efficient H_2 production.[73]

5. 3D High entropy alloy nanomaterials

3D geometry is pivotal in electrocatalysis due to its

influence on the spatial organization of matter at atomic and mesoscopic scales, which determines the density and accessibility of active sites, charge transport, and the diffusion of reactants and products. This significance is particularly pronounced in architected electrodes,[74] porous frameworks,[75] and crystalline catalysts with intricate 3D lattices such as open hollow nanoframes, cages and 3D ordered macroporous structures. Aerogels and xerogels also constitutes an important class of 3D structured materials explored for technologically important electrocatalytic reactions.[76] In these systems, geometric design can enhance catalytic performance by increasing surface exposure, reducing diffusion pathways, and improving electronic conductivity. Notable examples of three-dimensional structures include high-entropy alloys and ceramics, such as spinel, perovskite, rock-salt, fluorite, pyrochlore, and bixbyite oxides, as well as carbides, nitrides, and borides. These materials have garnered attention as electrocatalysts or catalyst supports for reactions including oxygen, hydrogen evolution, oxygen reduction, and carbon dioxide reduction.[77-79] 3D HEA nanomaterials consist of multiple elements in almost equal molar ratios. These materials are capable of forming complex microstructures or hierarchical architectures, e.g., nano-porous, foam-like, or microstructured forms. The 3D arrangement of these materials enhances their mechanical, thermal, and electrochemical properties. As a result, they are very well suited to a wide range of advanced applications.[80-84] An interesting synthesis of rosette-like high-entropy $NiCoFeMnAlO_x$ nanosheets (r-NCFMAO) through a straightforward hydrothermal method followed by annealing on nickel foam has been reported by Xu and coauthors.[85] This catalyst exhibits a porous, polycrystalline *fcc* spinel structure, which generates substantial interlayer voids, thereby enhancing substance diffusion and gaseous product evolution (Fig. 7A).[85] The high-entropy design, incorporating five distinct metal elements (Ni, Co, Fe, Mn, Al) in approximately equimolar ratios, increases the configurational entropy and optimizes the electronic structure through robust multi-element interactions. These properties confer an exceptionally high electrochemically active surface area and improved corrosion resistance, which are essential for maintaining structural stability in harsh seawater environments during extended electrolysis. The mechanistic pathways for plastic degradation, particularly for polyglycolic acid (PGA), involve the synergistic role of surface-generated OH* species that reduce activation energy barriers.[85] Detailed spectroscopic analysis using in-situ Raman and EPR revealed that OH* species are generated at low potentials and are rapidly consumed to drive the oxidation of organic intermediates. DFT calculations presented in [85] indicate that OH* species significantly lower the energy barrier for the rate-determining step, which involves the cleavage of the C-C bond in glyoxalate into formate and the subsequent activation of the C-H bond in formate into CO_2 / CO_3^{2-}. Importantly, the presence of the organic hydrolysate suppresses the chlorine oxidation reaction and outcompetes the oxygen evolution reaction (OER), enabling the catalyst to prioritize plastic degradation even in high chloride concentrations.[85] In terms of performance analysis, the r-NCFMAO catalyst demonstrated superior efficiency in both three-electrode cells and industrial-scale flow electrolyzers. In a standard electrochemical cell, the GA oxidation reaction achieved a current density of 100 mA cm^{-2} at only 1.36 V versus RHE, saving 190 mV compared to OER. When integrated into a paired GAOR || HER system, the electrolyzer reached an industrial-level current density of 1.0 A cm^{-2} at a low cell voltage of 1.96 V in natural alkaline seawater.[85] The system maintained stable operation for over 300 hours with 100% substrate conversion and a 90% CO_3^{2-} yield, ultimately enabling the recovery of 77% of the carbon as valuable $CaCO_3$. Furthermore, the catalyst exhibited broad applicability, degrading other plastics such as PET, PBS, PLA, and PBT with over 80% efficiency while consuming only ~3.8 kWh m^{-3} H2, which is lower than that of conventional water electrolysis (Fig. 7B).[85] Plastic degradation steps have been done in the simulated process roadmap displayed in (Fig. 7C) that shows the sequential stages, main chemical reactions, and key factors affecting the breakdown of plastics under controlled conditions.[85] The overall performance summary of high-entropy nanoalloys for electrocatalytic plastic waste upcycling is shown in **Table S1**.

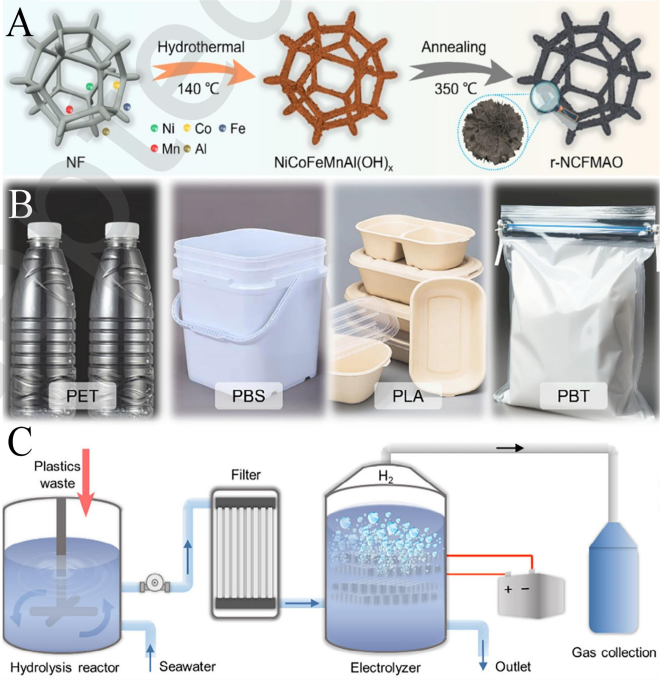

Fig. 7 (A) Diagram showing the synthesis of r-NCFMAO HEA. (B) Range of plastics (PET, PBS, PLA, and PBT) electrocatalytically degraded over r-NCFMAO HEA. (C) Illustration of the working flow for plastic degradation paired with H_2 evolution. Reproduced with permission from ref.[85] Copyright 2025, Wiley.

6. Noble metal-free HEAs

HEAs that incorporate earth-abundant, noble metal-free elements are emerging as viable, cost-efficient, and sustainable substitutes for traditional noble metal-based catalysts. These catalysts exploit the principle of high configurational entropy to create stable solid solutions from a variety of abundant metals, including iron, cobalt, nickel, copper, and manganese. Noble metal-free Noble metal free HEAs are likely to exhibit superior thermal and chemical stability in harsh environments, which is beneficial for long-term applications. Replacing scarce and costly noble metals with more readily available materials could substantially lower costs and reduce the environmental impact of catalytic processes.[86]

Although noble metal-free high entropy catalysts exhibit promising characteristics, they encounter several obstacles that limit their broader application. Matching the catalytic

performance of noble metals, especially in small organic molecule such as methanol, ethanol, ethylene glycol, glycerol and isopropanol oxidation is challenging due to typically lower intrinsic activity and selectivity, which requires precise tuning of composition and surface structures. The complexity of synthesis is another major concern, as variations in atomic size, electronic properties, and reactivity among the elements can cause phase segregation or inhomogeneity, negatively impacting catalytic efficiency.[86] Furthermore, non-noble metals are more susceptible to surface oxidation and catalyst deactivation under operational conditions, necessitating strategies to improve surface stability. The intricate atomic environments in these materials also complicate mechanistic understanding, hindering rational design and optimization. Progress in characterization and computational modeling is essential to overcoming these challenges and unlocking the full potential of noble metal-free high entropy catalysts.[87]

Linking HEA effects to electrocatalytic performance mechanistic framework

The cocktail effect facilitates multi-site synergism, where adjacent active sites with complementary roles influence the cleavage or retention of C–C bonds. In EGOR, HEAs rich in Pt/Pd promote C–C bond cleavage, resulting in CO_2 and acetic acid, whereas Cu/Ni-rich HEAs maintain C–C bonds, producing glycolic acid and lactate. The spacing of elements within HEAs (0.2–0.5 nm) dictates whether multi-carbon monomers fragment or retain their chain length. Lattice distortion (±3% strain) causes d-band modulation, shifting the d-band center by 0.1–0.3 eV compared to pure metals, thereby altering the adsorption energies of intermediates. A downward shift in the d-band weakens CO binding, reducing poisoning, while an upward shift enhances C=O adsorption, favoring oxidation to carboxylic acids. HEAs with a d-band center at −2.1 eV achieve 90% acetic acid selectivity from lactic acid, whereas a center at −1.8 eV results in 70% CO_2 production. This is influenced by specific elements. Au/Pt lower the d-band, while Ni/Fe elevate it. Severe lattice distortion (2–5% atomic-scale strain) generates heterogeneous binding sites that inhibit uniform CO/intermediate adsorption. The high-entropy effect reduces Gibbs free energy by 20–50 kJ/mol, thereby suppressing surface segregation during reactions exceeding 100 hours. Experimental evidence indicates that HEAs maintain less than 5% activity loss after 50 hours, compared to a 40% loss for PtNi binary alloys. The high-entropy effect also confers poisoning resistance; as sluggish diffusion prevents CO accumulation at active sites by a factor of 3–5 compared to conventional alloys. HEAs exhibit 10 times lower CO coverage at 0.5 V compared to Pt, enabling sustained ethylene glycol oxidation without deactivation.

7. Summary and perspectives

High-entropy alloy nanomaterials involve alloying multiple metal components to harness an unprecedented combination of properties, such as chemical stability, electrocatalytic activity, and mechanical strength. The freedom to select metallic compounds and combine them during synthesis results in a multi-component material with distinct characteristics that is so far not fully harnessed for purpose-driven applications such as electrochemical plastic hydrolysate catalysis. In this context, compositional space provided by HEA nanomaterials is exciting for the electrocatalytic community as it offers a credible way to control the activity, selectivity, and stability for a complex electrocatalytic process such as plastic hydrolysate catalysis that demands a group of seemingly incompatible panel of functionalities. Electrocatalytic plastic waste upcycling is a technologically important process as it helps in treatment of plastic waste through formation of value-added chemicals. Plastic hydrosylate is composed mostly of hydrocarbons and oxy-hydrocarbons depending on the type of polymer waste and component present in plastic waste mixture. Due to the inherent heterogeneity of plastic waste, the electrocatalytic upcycling process requires a robust electrode capable of simultaneously oxidizing different hydrocarbons. HEA nanomaterials can fulfill this specific requirement, as there is a large compositional and elemental space that can be tuned during HEA nanomaterial design and synthesis to produce HEA nanomaterials with desired catalytic functionality and stability.

The strategy of HEAs can extend beyond PET to encompass other hydrolyzable polyesters. However, its application is inherently restricted to polymers that can undergo depolymerization, rather than being applicable to all plastic types. The plastics most amenable to this approach include PET, polylactic acid (PLA), and other hydrolyzable polyesters such as poly(butylene succinate) (PBS), poly(butylene adipate-co-terephthalate) (AT), and polyglycolic acid (PGA). These plastics are suitable due to the presence of ester or other hydrolyzable bonds in their structure, which facilitate the initiation of electrocatalytic valorization through depolymerization into individual monomers. These monomers are generally water-soluble and can be processed under mild aqueous electrolysis conditions. Nonetheless, the HEA strategy encounters a significant limitation. It is ineffective for the majority of commercially available plastics, particularly polyethylene (PE) and polypropylene (PP), which constitute over 60% of global plastic waste. These polymers possess inert C–C backbones that resist hydrolysis and electrochemical activation under mild aqueous conditions, thereby hindering universal plastic valorization. The current strategy's reliance on hydrolyzable bonds precludes the direct cleavage of C–C/C–H bonds in these non-depolymerizable plastics. Future research must focus on developing catalysts capable of direct C–C/C–H bond cleavage under mild aqueous conditions to overcome these solid-state limitations and facilitate comprehensive plastic upcycling across all major plastic waste categories.

The reliance on critical metals necessitates a shift towards high-entropy alloys (HEAs) devoid of noble metals, such as Cu-Fe-Ni-Co-Zn, Co-Cr-Fe-Mn-Ni, and Fe-Ni-Cu-W-Ru. These alloys aim to reduce catalyst costs to below $50 per kilogram, a significant decrease from the current $500–2000 per kilogram for platinum-based catalysts. This involves minimizing the loading to under 1 mg cm^{-2} and implementing metal recovery loops with efficiencies exceeding 90%. To address catalyst reconstruction and leaching, it is essential to quantify metal dissolution, maintaining levels below 5 ppm/h, stabilize surfaces with 2–5 nm carbon or nitride coatings, monitor in-situ reconstruction through XAS/XPS, and ensure activity decay remains under 10% after 500 hours. Addressing the tolerance to real plastic additives and impurities requires testing with actual waste hydrolysates containing 1–5% additives, such as phthalates, BPA, Cl^-, and sulfur compounds. This involves developing HEA sites resistant to

poisons, with Au-rich sites for Cl^- and Ni-Fe sites for sulfur, and integrating pre-treatment processes to remove over 90% of impurities while maintaining more than 80% activity.

The integration of hydrolysis with electrolysis necessitates the development of one-pot tandem catalysts capable of performing both depolymerization and electrocatalysis. Electro-assisted hydrolysis should accelerate monomer release, allowing direct effluent linking without purification, and aim for a processing energy target of less than 2 kWh/kg, compared to the current 5–10 kWh/kg. At the reactor level, benchmarks involve scaling from laboratory conditions of 10–50 mA cm^{-2} to industrial conditions of 200–500 mA cm^{-2} in zero-gap or flow-cell electrolyzers. The future efforts should be aimed at achieving energy efficiency greater than 60%, compared to the current 30–40%, with a cell voltage of less than 2.5 V at 300 mA cm^{-2}, durability exceeding 500 hours, and a production cost of less than $0.8 per kilogram of acetic acid, making it competitive with fossil-based routes. The current laboratory state (6–50 hours of electrode stability) should be improved with a 5-year targets reaching 200–500 hours and industrial thresholds of over 1000 hours.

The analysis of literature reports summarized in this review article indicates that most HEA nanomaterials used for electrocatalytic upcycling contain at least one critical metal (less abundant due to supply or availability issues), such as Pt, Pd, Co, Ag, and Au. It is imperative to design and synthesise catalyst compositions avoiding critical elements without compromising the activity and stability. The electrooxidation of monomers derived from plastic hydrolysis involves intricate multi-electron pathways. Achieving high selectivity and efficiency necessitates precise tuning of the catalyst structure, the applied potential, and the electrolyte environment. There is a persistent need to enhance HEA catalyst stability during the processing of complex, real-world plastic feedstock, rather than pure laboratory samples. The efficacy of electrocatalysis using HEA nanomaterials is predominantly confined to hydrolyzable polyesters, such as PET and PLA, rather than to the more prevalent non-hydrolyzable plastics. New approaches should be developed to find ways to solubilize non-hydrolyzable plastics and further to upcycle them using electrocatalysis. Transitioning from laboratory research to practical application involves conducting scale-up experiments and designing electrolyzer components that can reliably function under industrial conditions (current densities >500 mA/cm^2). A sustained effort to develop HEA nanomaterials that can meet these demanding requirements is certainly needed to move this interesting and most promising technology to next level of development. Further, developing HEA catalysts capable of direct C–C/C–H bond cleavage under mild aqueous conditions is required for universal electrochemical plastic valorization.

Data availability

Not applicable.

Acknowledgements

This work was supported by the project MEBioSys with Reg. No. CZ.02.01.01/00/22_008/0004634, Co-funded by the ERDF as part of the MŠMT and funding received from the Technology Agency of the Czech Republic through the Delta 2 Program (Ref No. TM05000013).

Declaration of competing interest

All the contributing author(s) report(s) no conflict of interests in this work.

Author contribution statement

Palaniappan Subramanian: Data curation, project administration, validation, writing manuscript. **Palanisamy Kannan**: Data curation, project administration, validation, experimental design. **Jan Minar**: Project administration, funding acquisition. All the authors have approved the final manuscript.

Informed consent

Not applicable.

Ethics statement

Not applicable.

Use of AI statement

During the preparation of Figure 1, the author(s) used ChatGPT in order to assist with the graphical refinement and aesthetic outlook. After using this tool, the author(s) reviewed and edited the content as needed and take(s) full responsibility for the content of the publication."

References

[1] Nayanathara Thathsarani Pilapitiya PGC, Ratnayake AS. The world of plastic waste: A review. *Cleaner Mater.* **2024**, *11*, 100220.

[2] Singh N, Walker TR. Plastic recycling: A panacea or environmental pollution problem. *npj Mater. Sustain.* **2024**, *2*, 17.

[3] Salahuddin U, Sun J, Zhu C, Wu M, Zhao B, Gao P-X. Plastic recycling: A review on life cycle, methods, misconceptions, and techno-economic analysis. *Adv. Sustain. Syst.* **2023**, *7*, 2200471.

[4] Ma Y, Jiang X, Xiang X, Qu P, Zhu M. Recent developments in recycling of post-consumer polyethylene waste. *Green Chem.* **2025**, *27*, 4040-4093.

[5] Bernat K. Post-consumer plastic waste management: From collection and sortation to mechanical recycling. *Energies* **2023**, *16*, 3504

[6] Zhao X, Korey M, Li K, Copenhaver K, Tekinalp H, Celik S, Kalaitzidou K, Ruan R, Ragauskas AJ, Ozcan S. Plastic waste upcycling toward a circular economy. *Chem. Eng. J.* **2022**, *428*, 131928.

[7] Jehanno C, Alty JW, Roosen M, De Meester S, Dove AP, Chen EYX, Leibfarth FA, Sardon H. Critical advances and future opportunities in upcycling commodity polymers. *Nature* **2022**, *603*, 803-814.

[8] Roy PS, Garnier G, Allais F, Saito K. Strategic approach towards plastic waste valorization: Challenges and promising chemical upcycling possibilities. *ChemSusChem* **2021**, *14*, 4007-4027.

[9] Ogwu MC, Kosoe EA. Innovative approaches to recycling, upcycling, and downcycling for sustainable waste management. *CleanMat* **2025**, *2*, 242-261.

[10] Erickson ED, Tominac PA, Ma J, Aguirre-Villegas H, Zavala VM. Evaluating the economic and environmental benefits of deploying a national-scale, thermo-chemical plastic waste upcycling infrastructure in the United States. *Comp. Chem. Eng.* **2024**, *189*, 108800.

[11] Jan K, Deka D, Yu E, Lu T, Li K, Jiang H, Nawaz K, Webb E, Ozcan S, Zou R, Dai L, Lei H, Ruan R, Zhao X, Chen W-T. Recent advances in chemical recycling and upcycling of plastic waste into valuable materials, chemicals, and energy: a comprehensive review. *RSC Sustain.* **2026**, *4*, 1667-1702.

[12] Cai N, Xia S, Zhang X, Meng Z, Bartocci P, Fantozzi F, Chen Y, Chen H, Williams PT, Yang H. Preparation of iron-

and nitrogen-codoped carbon nanotubes from waste plastics pyrolysis for the oxygen reduction reaction. *ChemSusChem* **2020**, *13*, 938-944.
[13] Mir RA, Kaur G, Pandey OP. Facile process to utilize carbonaceous waste as a carbon source for the synthesis of low cost electrocatalyst for hydrogen production. *Inter. J. Hydrogen Energy* **2020**, *45*, 23908-23919.
[14] Mir RA, Pandey OP. Waste plastic derived carbon supported Mo_2C composite catalysts for hydrogen production and energy storage applications. *J. Clean Prod.* **2019**, *218*, 644-655.
[15] Upadhyay S, Mir RA, Kumar N, Pandey OP, Sen A. Reusing waste plastic bottle to reduce MoO_3 into carbon-supported MoO_2 nanoparticles for efficient water electrolysis. *Surf. Inter.* **2023**, *42*, 103297.
[16] Fan WK, Tahir M. Recent advances on cobalt metal organic frameworks (MOFs) for photocatalytic CO_2 reduction to renewable energy and fuels: A review on current progress and future directions. *Energy Convers. Manag.* **2022**, *253*, 115180.
[17] Mir RA, Singla S, Pandey OP. Hetero carbon structures derived from waste plastics as an efficient electrocatalyst for water splitting and high-performance capacitors. *Physica E: Low-dimens. Syst. Nanostruct.* **2020**, *124*, 114284.
[18] Kumar A, Sharma M, Sheoran S, Jaiswal S, Patra A, Bhattacharya S, Krishnan V. Tailoring defects in $SrTiO_3$ by one step nanoarchitectonics for realizing photocatalytic nitrogen fixation in pure water. *Nanoscale* **2023**, *15*, 11667-11680.
[19] Chand H, Sharma M, Krishnan V. Nanoarchitectonics of vanadium carbide MXenes for separation and catalytic degradation of contaminants. *Sep. Purif. Technol.* **2022**, *292*, 121032.
[20] Han M, Han M, Ma J, Du M, Zhu Q, Qiu B. Photocatalytic upcycling of plastic waste into value-added chemicals. *Electron* **2025**, *3*, e70005.
[21] Sajwan D, Sharma A, Sharma M, Krishnan V. Upcycling of plastic waste using photo-, electro-, and photoelectrocatalytic approaches: A way toward circular economy. *ACS Catal.* **2024**, *14*, 4865-4926.
[22] Xin Y, Li S, Qian Y, Zhu W, Yuan H, Jiang P, Guo R, Wang L. High-entropy alloys as a platform for catalysis: Progress, challenges, and opportunities. *ACS Catal.* **2020**, *10*, 11280-11306.
[23] Zhu Z, Li Z, Liu Z, Gu C, Zhang Q, Wang L. Advanced development of high-entropy alloys in catalytic applications. *Small Methods* **2026**, *10*, 2500411.
[24] Shi W, Liu H, Liu S, Chen J, Tan F, Wan J, Yao Y. Heterostructure engineering in high-entropy alloy catalysts. *SusMat* **2025**, *5*, e261.
[25] Hai A, Daud M, Mujtaba G, Banat F, Al-Harthi MA. A comprehensive review of two-dimensional high-entropy layered hydroxides: Synthesis, characterization, and applications. *Coord. Chem. Rev.* **2025**, *529*, 216435.
[26] Sun J, Liu W, Liang F, Liu R, Yao Y, Zou Q, Dong P, Wang S. Insight into high entropy compounds: Advances, challenges and energy applications. *Adv. Funct. Mater.* **2026**, *36*, e10855.
[27] Kc BR, Bastakoti BP. Rational design of high-entropy materials for photo and electrocatalytic applications. *Small Struct.* **2025**, *6*, 2500237.
[28] Jiménez-Arévalo VM, Martin P, Sepúlveda MF, Azocar MI, Zhou X, Galleguillos Madrid FM, Ramirez CG, Zagal JH, Páez M. Recent advances in high-entropy alloys for electrocatalysis: From rational design to functional performance. Mater. Des. 2025, 258, 114633.
[29] Guo B, Zhou Z, Sun W, Hu X. High entropy alloys for advanced electrocatalysis with computational insights and multidisciplinary design strategies. *iScience* **2025**, *28*, 113577.
[30] Wen Y, Jiang P, Ge B, Huang C, Ding K. High-entropy materials for electrocatalysis: From features to applications. *J. Alloys Compd.* **2026**, *1061*, 187299.
[31] Ren J-T, Chen L, Wang H-Y, Yuan Z-Y. High-entropy alloys in electrocatalysis: from fundamentals to applications. *Chem. Soc. Rev.* **2023**, *52*, 8319-8373.
[32] Zhang Y, Wang D, Wang S. High-entropy alloys for electrocatalysis: Design, characterization, and applications. *Small* **2022**, *18*, 2104339.
[33] Yan X, Zhou Y, Wang S. Nano-high entropy materials in electrocatalysis. *Adv. Funct. Mater.* **2025**, *35*, 2413115.
[34] Chen J, Ren L, Chen X, Wang Q, Chen C, Fan J, Wang S, Binas V, Shen S. Well-defined nanostructures of high entropy alloys for electrocatalysis. *Exploration* **2025**, *5*, 20230036.
[35] Pavithra CLP, Dey SR. Advances on multi-dimensional high-entropy alloy nanoarchitectures: Unconventional strategies and prospects. *Nano Select* **2023**, *4*, 48-78.
[36] Cui M, Zhang Y, Xu B, Xu F, Chen J, Zhang S, Chen C, Luo Z. High-entropy alloy nanomaterials for electrocatalysis. *Chem. Commun.* **2024**, *60*, 12615-12632.
[37] Kar N, Skrabalak SE. Synthetic methods for high-entropy nanomaterials. *Nat. Rev. Mater.* **2025**, *10*, 638-653.
[38] Zhao J-J, Zhu H-R, Huang C-J, Yin M-H, Li G-R. Recent advances of ethylene glycol oxidation reaction: catalytic mechanism, catalyst design and applications. *J. Mater. Chem. A* **2025**, *13*, 3236-3272.
[39] Ma Y, Han M, Qian Y, Xing D, Ma J, Yu Y, Qiu B, Zhang Y. Tandem depolymerization-electrocatalysis for plastic waste upcycling. *Green Chem.* **2026**, *28*, 96-119.
[40] Cho J, Kim B, Kwon T, Lee K, Choi S-I. Electrocatalytic upcycling of plastic waste. *Green Chem.* **2023**, *25*, 8444-8458.
[41] Liu L, Fan L, Zhang Y, Piao M, Du H. Addressing the plastic waste crisis: Advanced catalytic strategies for upcycling and fuel production. *Environ. Res.* **2025**, *284*, 122250.
[42] Ma X, Huang S, Jin Y, Jiang H, Tang L, Wu Y, Ni Y, Zhu S, Li X, Dietrich AM. Electrocatalytic dechlorination of aqueous trichloroacetic acid by Vitamin B12 modified iron electrode. *J. Environ. Chem. Eng.* **2023**, *11*, 109944.
[43] Zhou H, Ren Y, Li Z, Xu M, Wang Y, Ge R, Kong X, Zheng L, Duan H. Electrocatalytic upcycling of polyethylene terephthalate to commodity chemicals and H_2 fuel. *Nat. Commun.* **2021**, *12*, 4679.
[44] Wu H, Tian H, Chen L, Luo W, Li S, Wang L, Cui X, Shi J. Advances and insights in electrocatalytic upcycling of polyethylene terephthalate plastic wastes. *Adv. Mater.* **2026**, *38*, e15766.
[45] Li J, Chen J, Zhang L, Matos J, Wang L, Yang J. Electrocatalytic upcycling of plastic waste: Progress, challenges, and future. *Electron* **2024**, *2*, e63.
[46] Wang G, Chen Z, Wei W, Ni B-J. Electrocatalysis-driven sustainable plastic waste upcycling. *Electron* **2024**, *2*, e34.
[47] Wang K, Huang J, Chen H, Wang Y, Yan W, Yuan X, Song S, Zhang J, Sun X. Recent progress in high entropy alloys for electrocatalysts. *Electrochem. Energy Rev.* **2022**, *5*, 17.
[48] Cai J, Zhu H. Surface-engineered nanostructured high-entropy alloys for advanced electrocatalysis. *Commun. Mater.* **2025**, *6*, 118.

[49] Kuang L-F, Zhang L, Li H, Qin H-Y, Chi H-Z, Liu J-B, Zhang J, Yan F, Xiao X-Z. Recent progress in high-entropy nanocatalysts. *cMat* **2024**, *1*, e26.
[50] Wang H, Kang X, Han B. Optimizing CO2 electroreduction: theoretical insights for enhancing efficiency across elementary steps. *Chem. Soc. Rev.* **2025**, *54*, 10156-10244.
[51] Hameed A, Javed S, Tariq I, Li P, Nadeem MA, Jin R. High-entropy materials as catalysts for alcohol and polyol electro-oxidation: Advances, mechanisms, and future perspectives. *ACS Catal.* **2026**, *16*, 1802-1831.
[52] Xu D, Wang X, Lu Y. Heterogeneous-structured refractory high-entropy alloys: A review of state-of-the-art developments and trends. *Adv. Funct. Mater.* **2024**, *34*, 2408941.
[53] Tam Nguyen T, Edalati K. Efficient photoreforming of plastic waste using a high-entropy oxide catalyst. J. Catal. 2024, 440, 115808.
[54] Wu F, Dou Y, Zhou J, Qin J, Jiang T, Yao Y, Hélix-Nielsen C, Zhang W. High-entropy (FeCoNiCuZn)WO_4 photocatalysts-based fibrous membrane for efficient capturing and upcycling of plastic. *Chem. Eng. J.* **2023**, *470*, 144134.
[55] Wang X, Liu Q, Wang X. High-entropy materials: From bulk to sub-nano. *Adv. Funct. Mater.* **2025**, *35*, 2504275.
[56] Adhikari J, Saha P, Mandal P, Sinha SK, Seikh AH, Mohammed JA, Ghosh M. A review on high entropy alloys as metallic biomaterials: Fabrication, properties, applications, challenges, and future prospects. *Biomed. Mater. Dev.* **2026**, *4*, 1190-1219.
[57] Chen S-T, Wang L, Hou H-E, Wang K-S, Lan Z, Yang Y-Y, Cai W-B. PtBiCoAgSn multi-component alloy electrocatalysts enhancing the oxidation of ethylene glycol to value-added C_2 products. *Molecules* **2025**, *30*, 3872
[58] Zheng Q, Huang L, Yang S, Liang Q, Yang Y, Gu L, Cheng R, Shen Y, Yan Z, Cao X. Synergy between multi-components and Ir dopant in Ir-doped high-entropy alloy nanoparticles for efficient and robust ethylene glycol electro-oxidation at an industrial-level current. *Nanoscale* **2025**, *17*, 12989-12999.
[59] Dong Y, Zhang L, Wu T, Zhan Y, Zhou B, Wei F, Zhang D, Long X. Multi-dimensional high-entropy materials for energy conversion reactions: Current state and future trends. *ChemSusChem* **2025**, *18*, e202401261.
[60] Li J, Zhang Y, Wei H, Ma T, Liu F, Hu F, Xu W, Tao Z, Xia S, Cui Q, Wang N, Wei H. 0D/1D confinement engineering and high-entropy coordination enable electrocatalytic industrial-grade hydrogen production. *Compos. Part B: Eng.* **2026**, *309*, 113083.
[61] Chang L, Jing H, Liu C, Qiu C, Ling X. High-entropy materials for prospective biomedical applications: Challenges and opportunities. *Adv. Sci.* **2024**, *11*, 2406521.
[62] Hao J, Wang T, Cai J, Gao G, Zhuang Z, Yu R, Wu J, Wu G, Lu S, Wang X, Du M, Wang D, Zhu H. Suppression of structural heterogeneity in high-entropy intermetallics for electrocatalytic upgrading of waste plastics. *Angew. Chem. Inter. Ed.* **2025**, *64*, e202419369.
[63] Geng R, Wei R, Zhang X, Zhang Z, Wang Y, Li G, Yin S. Multisite synergism-induced electron regulation of high-entropy alloy nanowires for electrocatalytic reforming of polylactic acid plastic hydrolysate. *J. Mater. Chem. A* **2026**, *14*, 2179-2187.
[64] Xiang Q, Chen F, Zhou Y, Pan X, Zhu H. Phosphorus doping in high-entropy carbides promotes the selectivity in electrooxidation of ethylene glycol to formic acid. *New J. Chem.* **2025**, *49*, 7553-7559.
[65] Lu D, Fu X, Guo D, Ma W, Sun S, Shao G, Zhou Z. Challenges and opportunities in 2D high-entropy alloy electrocatalysts for sustainable energy conversion. *SusMat* **2023**, *3*, 730-748.
[66] Qiu Z, Li Y, Gao Y, Meng Z, Sun Y, Bai Y, Suen N-T, Chen H-C, Pi Y, Pang H. 2D MOF-assisted pyrolysis-displacement-alloying synthesis of high-entropy alloy nanoparticles library for efficient electrocatalytic hydrogen oxidation. *Angew. Chem. Inter. Ed.* **2023**, *62*, e202306881.
[67] Fan L, Wang C, Wang J, Xin Y, Wu Y, Fan Z, Yang L-M, Zhang Z. Ambient laser writing of strongly coupled high-entropy alloy nanohybrids for peroxide electrocatalysis and on-chip dual-mode sensing. *Adv. Funct. Mater.* **2025**, *36*, e28977.
[68] Chandio I, Jiao Q, Li R, Ai Y, Liang Q. Dual-signal electrochemical aptasensor based on high-entropy alloy nanosheets for calprotectin detection in inflammatory bowel disease. *ACS Appl. Mater. Inter.* **2025**, *17*, 38960-38970.
[69] Wang W, Xiao N, Yang R, Lin H, Deng K, Wang J, Wang H, Yu H, Wang L. High-entropy metallene arrays with a turing structure for electrocatalytic upcycling of polyethylene terephthalate plastics coupled with electrosynthesis of ammonia. *ACS Nano* **2025**, *19*, 28675-28689.
[70] Wang Z, Lin H, Wang W, Yu H, Xu Y, Deng K, Wang H, Wang L. High-entropy PdPtRhFeCuMo metallene nanoribbons for electro-reforming PET plastic into glycolic acid. *Chin. J. Struct. Chem.* **2025**, *44*, 100745.
[71] Xiao N, Jiang S, Wang Z, Deng K, Xu Y, Yin S, Wang H, Wang L, Yu H. Orbital-hybridization-induced intermediate stabilization on turing high-entropy metallene for electrocatalytic polyethylene terephthalate valorization coupled with hydrogen evolution. *Chem. Eng. J.* **2026**, *527*, 171937.
[72] Wang Z, Chen J, Wang Y, Yu H, Xu Y, Deng K, Wang H, Wang L. Synergistic electronic effect in high-entropy PdPtSnBiAg metallene for electrochemical reforming of PET plastic into glycolic acid. *J. Mater. Chem. A* **2025**, *13*, 37178-37184.
[73] Zhou Y, Tian T, Jiang S, Shen R, Yu H, Wang Z, Wang H, Wang L, Deng K. Alternating pulse driven periodic reactivation of high-entropy mesoporous film boosts continuous membrane-free PET waste upcycling coupled with H2 production. *Adv. Funct. Mater.* **2026**, *36*, e11835.
[74] Ren Q, Feng L, Tran C, Eisenberg S, Xue X, Pinongcos A, Duoss EB, Zhu C, Li Y. Interpenetrating 3D electrodes for high-rate alkaline water splitting. *ACS Mater. Lett.* **2024**, *6*, 3705-3712.
[75] Yu X, Zhang Y, Li H, Wang R, Liu H, Wang J, Lin Y, Li Z. Multifunctional crystalline porous polymers for advanced electrocatalysis. *Trends Chem.* **2026**, *8*, 319-335.
[76] Mladenović D, Samancı M, Santos DMF, Bayrakçeken A, Šljukić B. Carbon aerogel and xerogel composites with polypyrrole as electrocatalysts for oxygen reduction reaction. *Surf. Inter.* **2025**, *60*, 106071.
[77] Liu Y, Zhang Y, Sun Z, Dai L, Liu B, Li W. Catalysts with three-dimensional porous structure for electrocatalytic water splitting. *Sustain. Mater. Technol.* **2025**, *44*, e01392.
[78] Xu J, Ma Y, Xuan C, Ma C, Wang J. Three-dimensional electrodes for oxygen electrocatalysis. *ChemElectroChem* **2022**, *9*, e202101522.
[79] Wang X, Liu X-j, Wang D, Rui-tang G. From 0D to 3D: Carbon-based materials and their electrocatalytic CO_2 reduction performance. *iScience* **2026**, *29*, 115631.
[80] Lin C-Y, He ZY, Lin J-T, Chang C-W, Hsiao Y-C, Lin S-C, Chen Y, Huang Y-M, Lee S-C, Pao C-W, Lin K-H, Cowan AJ,

Yang T-H. Atomically mixed high-entropy-alloy nanoframes with 3D subnanometer-thick electrocatalytic surfaces. *Adv. Funct. Mater.* **2025**, *35*, 2505927.
[81] Fan W, Li Z, Zhang J, Song Y, Zhang S, Liu C, Han S, Dong Y, Xu Z, Hong N, Kang J, Wang S, Yang Z, Li N, Wang Z. Flash Joule heating-enhanced in-situ synthesis of 3D graphene/high-entropy alloy composites for efficient electromagnetic wave absorption. *Carbon* **2025**, *243*, 120561.
[82] Lin X, Hu Y, Hu K, Lin X, Xie G, Liu X, Reddy KM, Qiu H-J. Inhibited surface diffusion of high-entropy nano-alloys for the preparation of 3D nanoporous graphene with high amounts of single atom dopants. *ACS Mater. Lett.* **2022**, *4*, 978-986.
[83] Miao W. Dual-signal amplification via high-entropy alloy nanoparticle catalysis and target DNA recycling for ultrasensitive HPV-16/18 detection in human serum. *Sens. Actuat. B: Chem.* **2026**, *448*, 138927.
[84] Chandio I, Cheung S, Ai Y, Liang Q. High-entropy alloy nanoparticles integrated with metal-organic framework for enhanced aptasensing of carcinoembryonic antigen. *Microchem. J.* **2025**, *209*, 112760.
[85] Xu Z, Wang Y, Zheng Z, Zhang X, Liu B, Wilson K, Yan K. Electrochemical degradation of plastic waste coupled with hydrogen evolution in seawater using rosette-like high-entropy oxides. *Adv. Sci.* **2025**, 12, e07023.
[86] Huang H, Zhao J, Guo H, Weng B, Zhang H, Saha RA, Zhang M, Lai F, Zhou Y, Juan R-Z, Chen P-C, Wang S, Steele JA, Zhong F, Liu T, Hofkens J, Zheng Y-M, Long J, Roeffaers MBJ. Noble-metal-free high-entropy alloy nanoparticles for efficient solar-driven photocatalytic CO_2 reduction. *Adv. Mater.* **2024**, *36*, 2313209.
[87] Zhu J, Yu X, Guo M, Chen Z, Ni B-J. Design frontiers of high-entropy materials for advanced electrocatalysis. *Adv. Funct. Mater.* **2026**, *36*, e22077.

Electronic Supplementary Material

High entropy nanoalloys for electrocatalytic plastic waste upcycling

Palaniappan Subramanian[1], Palanisamy Kannan[2], and Jan Minar[1]

[1] *New Technologies – Research Center, University of West Bohemia in Pilsen, 30100, Czech Republic*
[2] *College of Biological, Chemical Sciences and Engineering, Jiaxing University, Jiaxing 314001, China*

Address correspondence to Palaniappan Subramanian, palans@ntc.zcu.cz; Palanisamy Kannan, ktpkannan@zjxu.edu.cn

Supporting information to https://doi.org/10.26599/NR.2026.94908996

Table S1. Performance of high-entropy nanoalloys for electrocatalytic plastic waste upcycling.

S.No.	Catalysts	Plastic Source	Substrate	Cell Type	Carbon Balance	Onset/potential @ current density	Product selectivity and FE	Demonstrated Stability	Ref.
1	Multi-Component alloy PtBiCoAgSn catalyst	Model substrate	1 M KOH + 1 M EG solution	3-electrode	NA	0.36 V vs. RHE 16.65 A mg^{-1}	GA 91%	1 hour	[1]
2	Ir-PdPtAuNiCu HEANs	Model substrate	1 M NaOH + 0.5 M EG solution	2-electrode electrolysis	NA	0.245 V vs. RHE 2.41 A mg^{-1} Pt+Pd^{-1}	GA 88.8%	1200 hours	[2]
3	$L1_0$-PtIrFeMoBi HEA NPs	Model substrate	1 M KOH + 1 M EG solution	H-type cell	NA	0.35 V vs. RHE 208.2 mA cm^{-2}	GA 95%	30 hours	[3]
4	HEA-AuCuAgPtNi nanowires	Model substrate	1 M KOH + 1 M LA solution	3-electrode	NA	1.35 V vs. RHE 56.2 mA cm^{-2}	AA 90.72%	10 hours	[4]
5	P-HEC NPs	Model substrate	1 M KOH + 2.4 M EG solution	3-electrode	NA	1.28 V vs. RHE 50 mA cm^{-2}	FA 89.25%	40 hours	[5]
6	PdPtCu-NiAg MARs	PET	1 M KOH + PET hydrolysate	Electrolyzer	NA	0.40 V vs. RHE 400 mA cm^{-2}	GA 95.8%	120 hours	[6]
7	PdPtRhFeCuMo HMRs	Model substrate	1 M KOH + 1 M EG solution	H-type cell	NA	0.36 V vs. RHE 280 mA cm^{-2}	GA 96.81%	24 hours (12 two hour cycles)	[7]
8	Turing HEA-PdPtCuNiBiene	PET	1 M KOH + PET hydrolysate	Electrolyzer cell	NA	0.28 V vs. RHE 400 mA cm^{-2}	GA 96%	30 hours	[8]
9	HEA-PdPtSnBiAg metallene	PET	1 M KOH + PET hydrolysate	2-electrode electrolysis	NA	0.37 V vs. RHE 210.07 mA cm^{-2}	GA 91.8%	12 hours (6 two hour cycles)	[9]
10	m-HEA (Pd-Cu-Au-Ag-Pt) /NF	PET	1 M KOH + PET hydrolysate	Electrolyzer cell	NA	0.50 V vs. RHE 250 mA cm^{-2}	GA 91%	100 hours of alternating pulse	[10]
11	HEA-NiCoFeMnAlO_x nanosheets	PET, PLA, PBS, PBT	1 M KOH + 1 M GA solution	Electrolyzer cell	97%	1.20 V vs. RHE 400 mA cm^{-2}	GA 85%	300 hours	[11]

References

[1] Chen S-T, Wang L, Hou H-E, Wang K-S, Lan Z, Yang Y-Y, Cai W-B. PtBiCoAgSn multi-component alloy electrocatalysts enhancing the oxidation of ethylene glycol to value-added C_2 products. *Molecules* **2025**, *30*, 3872

[2] Zheng Q, Huang L, Yang S, Liang Q, Yang Y, Gu L, Cheng R, Shen Y, Yan Z, Cao X. Synergy between multi-components and Ir dopant in Ir-doped high-entropy alloy nanoparticles for efficient and robust ethylene glycol electro-oxidation at an industrial-level current. *Nanoscale* **2025**, *17*, 12989-12999.

[3] Hao J, Wang T, Cai J, Gao G, Zhuang Z, Yu R, Wu J, Wu G, Lu S, Wang X, Du M, Wang D, Zhu H. Suppression of structural heterogeneity in high-entropy intermetallics for electrocatalytic upgrading of waste plastics. *Angew. Chem. Inter. Ed.* **2025**, *64*, e202419369.

[4] Geng R, Wei R, Zhang X, Zhang Z, Wang Y, Li G, Yin S. Multisite synergism-induced electron regulation of high-entropy alloy nanowires for electrocatalytic reforming of polylactic acid plastic hydrolysate. *J. Mater. Chem. A* **2026**, *14*, 2179-2187.

[5] Xiang Q, Chen F, Zhou Y, Pan X, Zhu H. Phosphorus doping in high-entropy carbides promotes the selectivity in electrooxidation of ethylene glycol to formic acid. *New J. Chem.* **2025**, *49*, 7553-7559.

[6] Wang W, Xiao N, Yang R, Lin H, Deng K, Wang J, Wang H, Yu H, Wang L. High-entropy metallene arrays with a turing structure for electrocatalytic upcycling of polyethylene terephthalate plastics coupled with electrosynthesis of ammonia. *ACS Nano* **2025**, *19*, 28675-28689.

[7] Wang Z, Lin H, Wang W, Yu H, Xu Y, Deng K, Wang H, Wang L. High-entropy PdPtRhFeCuMo metallene nanoribbons for electro-reforming PET plastic into glycolic acid. *Chin. J. Struct. Chem.* **2025**, *44*, 100745.

[8] Xiao N, Jiang S, Wang Z, Deng K, Xu Y, Yin S, Wang H, Wang L, Yu H. Orbital-hybridization-induced intermediate stabilization on turing high-entropy metallene for electrocatalytic polyethylene terephthalate valorization coupled with hydrogen evolution. *Chem. Eng. J.* **2026**, *527*, 171937.

[9] Wang Z, Chen J, Wang Y, Yu H, Xu Y, Deng K, Wang H, Wang L. Synergistic electronic effect in high-entropy PdPtSnBiAg metallene for electrochemical reforming of PET plastic into glycolic acid. *J. Mater. Chem. A* **2025**, *13*, 37178-37184.

[10] Zhou Y, Tian T, Jiang S, Shen R, Yu H, Wang Z, Wang H, Wang L, Deng K. Alternating pulse driven periodic reactivation of high-entropy mesoporous film boosts continuous membrane-free PET waste upcycling coupled with H_2 production. *Adv. Funct. Mater.* **2026**, *36*, e11835.

[11] Xu Z, Wang Y, Zheng Z, Zhang X, Liu B, Wilson K, Yan K. Electrochemical degradation of plastic waste coupled with hydrogen evolution in seawater using rosette-like high-entropy oxides. *Adv. Sci.* **2025**, *12*, e07023.